

ADAPTIVE EXPERIMENTAL DESIGN APPLIED TO AN ERGONOMICS TESTING PROCEDURE

Michael Sasena,¹ Matthew Parkinson,² Pierre Goovaerts,³ Panos Papalambros,⁴ Matthew Reed⁵

University of Michigan

Ann Arbor, Michigan 48109

{msasena, mparkins, goovaert, pyp, mreed}@umich.edu

ABSTRACT

Nonlinear constrained optimization algorithms are widely utilized in artifact design. Certain algorithms also lend themselves well to design of experiments (DOE). *Adaptive design* refers to experimental design where determining where to sample next is influenced by information from previous experiments. We present a constrained optimization algorithm known as superEGO (a variant of the EGO algorithm of Schonlau, Welch and Jones) that is able to create adaptive designs effectively. Its ability to allow easily for a variety of sampling criteria and to incorporate constraint information accurately makes it well suited to the needs of adaptive design. The approach is demonstrated on a human reach experiment where the selection of sampling points adapts successfully to the stature and perception of the individual test subject. Results from the initial study indicate that superEGO is able to create experimental designs that yield more accurate models using fewer points than the original testing procedure.

NOMENCLATURE

DOE Design of Experiments

ISC Infill Sampling Criterion

MLE Maximum Likelihood Estimation

SCF Spatial Correlation Function

$\hat{y}(\mathbf{x})$ Kriging estimate of y at \mathbf{x}

$\hat{s}^2(\mathbf{x})$ Kriging variance of y at \mathbf{x}

$R(\mathbf{w}, \mathbf{x})$ Spatial Correlation between \mathbf{w} and \mathbf{x}

\mathbf{R} sample to sample correlation matrix

\mathbf{r}_x Sample to prediction point correlation vector

σ^2 Process variance

$\hat{\beta}$ Global trend of the kriging model

θ Kriging model parameter to be fit

p Kriging model parameter to be fit

nugget Kriging model parameter to be fit (controls smoothing)

d Number of input variable dimensions

n Number of sample points

g_i Constraint function i

INTRODUCTION

An experimental run, be it a physical experiment or done on a computer, can be viewed as a black-box function. Input values are sent to the black-box, and the associated outputs are returned. Design of experiments (DOE) studies how to select the set of input values at which to evaluate the black-box in order to explore its behavior efficiently. There are many ways to quantify how well a particular design achieves that goal. Among the most frequently used are factorial and composite designs, Latin hypercubes and orthogonal arrays. Each strategy attempts to spread points around the design space in some appropriate manner. The reader is referred to Montgomery (1997) for more background on classical design of experiments.

¹Ph.D. Candidate, Department of Mechanical Engineering

²Ph.D. Pre-Candidate, Department of Biomedical Engineering

³Assistant Professor, Department of Civil and Environmental Engineering

⁴Professor, Department of Mechanical Engineering

⁵Assistant Research Scientist, UofM Transportation Research Institute

In some applications, a particularly useful approach is to determine the set of input values sequentially, taking into account information from the previous experiments. These so-called *adaptive designs* can be performed either in stages, where several new inputs are chosen at each stage, or fully adaptively, where each new input incorporates all prior information. Adaptive designs often appear in such fields as clinical research or allocation problems. For example, one class of problems known as *bandit problems* seeks to choose points from a finite set of alternative experiments with unknown outcomes at each of n stages in order to maximize overall yield. Clinical trials may use adaptive designs to determine whether to assign a test subject to the control or study group based upon the data collected thus far (Zacks, 1996).

Adaptive designs are generally more complicated to generate because they require an optimization problem to be solved each time new input values are chosen rather than fixing the entire DOE before the experiments begin. The topic is currently an active area of research (Thompson and Seber, 1996), (Flourney et al., 1997), (Atkinson et al., 1998 and 2001) and specialized algorithms have been developed (Hardwick and Stout, 1998). However, because adaptive design involves solving an optimization problem, general nonlinear programming techniques can be used to generate the designs.

The framework used here to create adaptive designs is a constrained nonlinear optimization algorithm known as *superEGO* (Sasena et al., 2001 and 2002), (Sasena, 2002), a variation of the EGO algorithm of Schonlau, Welch and Jones (Schonlau, 1997). It belongs to a class of optimization algorithms known as Bayesian analysis, which work by taking an initial sample and fitting an approximation to the data. In the case of EGO and superEGO, the approximation consists of a kriging model (Goovaerts, 1997). Some infill sampling criterion (ISC) is then numerically maximized in order to determine where to evaluate the functions next. The kriging models are iteratively updated with the new samples until the termination criterion is reached (e.g., the maximum number of samples is reached). The flowchart of the superEGO algorithm is shown in Figure 1.

To demonstrate superEGO's search strategy for traditional optimization problems, a one dimensional multimodal example is shown in Figure 2. The w-shaped dashed line is the true objective function we wish to minimize, while the solid line is the kriging approximation conditional to the sample points shown as circles. The plot at the bottom is the sampling criterion, normalized to facilitate comparisons between iterations. Observing the progression of the algorithm, one can see that it searches for the optimum by looking for points of good local improvement as well as regions of high model uncertainty where there is a possibility of an overlooked optimum. After the initial sample of 4 points is taken, the resulting kriging model is a poor fit compared to the true function. However, the ISC leads the algorithm to sample points where the uncertainty in the model is highest.

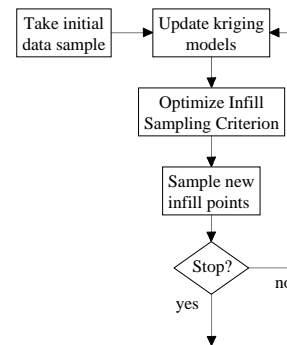


Figure 1. Flowchart of the superEGO algorithm

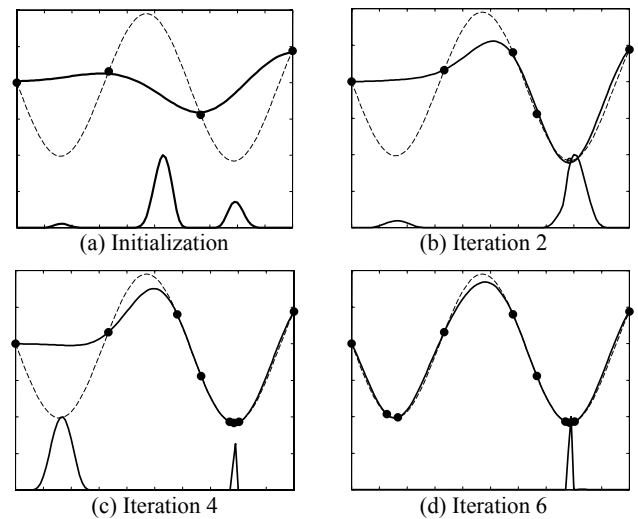


Figure 2. Demonstration of superEGO. Dashed line is the true function to be minimized, solid line is the approximation, circles are the sample points. The plot at the bottom is the sampling criterion.

After two iterations, the model has improved in the region of the local optimum on the right. Two iterations later, the region on the left has been explored somewhat, but the uncertainty in the model on the left portion of the model drives superEGO to sample points in that region. After six iterations, both local optima have been discovered and the true solution has been found quite accurately.

The search behavior is controlled by the choice of sampling criterion. SuperEGO can use any one of 16 predefined criteria due to its flexible framework. The user can also define a new criterion quite easily. In the above example, the expected improvement function (Schonlau, 1997) was used as the ISC in order to locate the minimum of the test function. Instead of locating the constrained minima of the function, superEGO can be used to generate adaptive design of experiments simply by defining an

appropriate sampling criterion.

In much of the research on adaptive sampling, measures such as the integrated mean squared error or maximum mean squared error are used as the criterion for selecting the next sample point (Sacks et al., 1989a and 1989b). The study presented later in this work takes advantage of the flexibility of superEGO by defining sampling criteria designed specifically for this application. In addition, superEGO is able to incorporate constraint information directly into the auxiliary problem of optimizing the ISC such that it prevents infeasible regions from being sampled. This is quite important as the constraints placed upon the sampling scheme are there to prevent injury to the test subject. Jones' DIRECT algorithm (Jones et al., 1993), (Jones, 2001) was used to solve the resulting auxiliary constrained global optimization problem.

The remainder of the paper is organized as follows. We begin by briefly describing kriging and its application in this work. We then describe the application study, a test procedure for an ergonomics experiment. The methods used to address the problems are explained, and the results are shown. We conclude by highlighting the contributions in this work and possible avenues for future research.

AN OVERVIEW OF KRIGING

We begin this section with an introduction to the approximation method used. Much of the explanation follows Schonlau's derivation (1997). Next, we describe a method for fitting models that are non-interpolating.

Kriging Formulae

There has been much interest lately in a form of curve fitting and prediction known as kriging. Originally developed for use in mining and soil sciences in the 1950's, it grew into the field of study called geostatistics. In the late 1980's, statisticians introduced Design and Analysis of Computer Experiments (DACE) by adapting the kriging techniques to deterministic, simulation-based data (Sacks et al., 1989b). This work, like most kriging applications outside of the civil and environmental engineering, uses the DACE approach to kriging.

A kriging metamodel, which takes the form $Y(\mathbf{x}) = f(\mathbf{x}) + Z(\mathbf{x})$, is comprised of two parts: a polynomial $f(\mathbf{x})$ and a functional departure from that polynomial $Z(\mathbf{x})$. We will assume a constant term polynomial, that is $f(\mathbf{x}) = \beta$. This simplification is often used and provides sufficiently accurate results because of the flexibility of $Z(\mathbf{x})$ (Sacks et al., 1989a). More precisely, $Z(\mathbf{x})$ represents uncertainty in the mean of $Y(\mathbf{x})$ with $E(Z(\mathbf{x})) = 0$ and

$$\text{Cov}(Z(\mathbf{w}), Z(\mathbf{x})) = \sigma^2 R(w, x), \quad (1)$$

where σ^2 is a scale factor (the process variance) that can be tuned

to the data, and $R(\mathbf{w}, \mathbf{x})$ is known as the spatial correlation function (SCF).

The choice of the SCF determines how the metamodel fits the data. There are many choices of $R(\mathbf{w}, \mathbf{x})$ to quantify how quickly and how smoothly the function moves from point \mathbf{x} to point \mathbf{w} . One of the most common SCF's (shown here for one-dimensional points w and x) used in DACE is

$$R(w, x) = e^{-\theta|w-x|^p}, \quad (2)$$

where $\theta > 0$ and $0 < p \leq 2$. As with all choices of SCF, the function tends to zero as $|w-x|$ increases.

To extend the SCF to several dimensions, common practice is to multiply the correlation functions. The so-called *product correlation rule* applied to Equation (2) results in

$$R(\mathbf{w}, \mathbf{x}) = \prod_{k=1}^d e^{-\theta^k |w^k - x^k|^p}, \quad (3)$$

where the superscript $k = 1$ to d refers to the dimension.

For n sample points, let \mathbf{R} be the $n \times n$ correlation matrix with element i, j defined by $R(\mathbf{x}_i, \mathbf{x}_j)$ as in Equation (3) and let

$$\mathbf{r}_x = [R(\mathbf{x}_1, \mathbf{x}), R(\mathbf{x}_2, \mathbf{x}), \dots, R(\mathbf{x}_n, \mathbf{x})]^t \quad (4)$$

be the $n \times 1$ vector of correlations between the point at which to predict, \mathbf{x} , and all the previously sampled data points \mathbf{x}_i . We can now define the kriging prediction equation as

$$\hat{y}(\mathbf{x}) = \hat{\beta} + \mathbf{r}_x^t \mathbf{R}^{-1}(\mathbf{y} - \mathbf{1}\hat{\beta}), \quad (5)$$

where \mathbf{y} is the vector of sampled output data, $\mathbf{1}$ is a vector of ones, and

$$\hat{\beta} = (\mathbf{1}^t \mathbf{R}^{-1} \mathbf{1})^{-1} \mathbf{1}^t \mathbf{R}^{-1} \mathbf{y} \quad (6)$$

is the generalized least squares estimator of β .

A very useful feature of kriging is the availability of the *kriging variance*, an estimate of the uncertainty in the prediction of $\hat{y}(\mathbf{x})$.

$$\text{MSE}[\hat{y}(\mathbf{x})] \equiv \hat{s}^2(\mathbf{x}) = \hat{\sigma}^2 (1 - \mathbf{r}_x^t \mathbf{R}^{-1} \mathbf{r}_x), \quad (7)$$

where $\hat{\sigma}^2$ is the generalized least squares estimator of the process variance of Equation (1) computed as

$$\hat{\sigma}^2 = \frac{1}{n} (\mathbf{y} - \mathbf{1}\hat{\beta})^t \mathbf{R}^{-1} (\mathbf{y} - \mathbf{1}\hat{\beta}). \quad (8)$$

The most difficult aspect of kriging is fitting the model parameters (θ and p) that describe the covariance function of Equation (3). In the DACE approach, models are fit with maximum likelihood estimation (MLE) by numerically minimizing the equation

$$\text{MLE} = \frac{1}{n} (n \ln \hat{\sigma}^2 + \ln(\det \mathbf{R})) , \quad (9)$$

which is a function of only the model parameters.

Smoothed Kriging Models

The approach to kriging described above results in an interpolating surface. That is, at the sampled data locations, the predictor goes exactly through the data, and the kriging variance returns to zero. While this is appropriate for many engineering applications, there are cases where a non-interpolating version of the kriging model would be very beneficial – for example, when the data are highly noisy. To allow kriging to smooth the data, an additional parameter is introduced into the SCF of Equation (3) to account for the measurement error, $E(\mathbf{x})$. The kriging model now takes the form $Y(\mathbf{x}) = f(\mathbf{x}) + Z(\mathbf{x}) + E(\mathbf{x})$, and the SCF appears as

$$R(\mathbf{w}, \mathbf{x}) = (1 - \text{nugget}) \prod_{k=1}^d e^{-\theta^k |w^k - x^k|^{p^k}} , \quad (10)$$

with $0 \leq \text{nugget} < 1$. The name refers to the *nugget effect* model used in geostatistics to describe the discontinuity of the covariance function as $|w - x|$ approaches zero. The scaling factor $(1 - \text{nugget})$ is the same as the ratio $\sigma_Z^2 / (\sigma_Z^2 + \sigma_E^2)$ defined in the DACE literature (Sacks et al., 1989a), (Sacks et al., 1989b). In either case, the additional parameter ranges between 0 and 1 and must be fit via MLE along with θ and p . We prefer the notation shown in Equation (10) simply because it is easier to view the value of *nugget* which is usually quite close to zero (e.g., 1e-5) rather than $\sigma_Z^2 / (\sigma_Z^2 + \sigma_E^2)$ which is usually quite close to 1 (e.g., 0.99999). Typically, a single scaling factor is applied to the covariance model. It is, however, possible to fit a separate *nugget* parameter for each dimension as

$$R(\mathbf{w}, \mathbf{x}) = \prod_{k=1}^d (1 - \text{nugget}^k) e^{-\theta^k |w^k - x^k|^{p^k}} , \quad (11)$$

so that more smoothing is applied in some directions than others.

A *nugget* value of zero means that the predictor goes exactly through the data. Increasing the *nugget* value results in smoothed models because collocated points no longer have perfect correlation. It is important to note that the scaling factor $(1 - \text{nugget})$

is *not* applied to the diagonal of the \mathbf{R} matrix, and *is* applied to the entire \mathbf{r}_x vector even when a prediction point coincides with a sample point. This is done because a point is perfectly correlated with itself (diagonal of \mathbf{R} matrix consists of ones), but would not be perfectly correlated with a second sample point at the same location (\mathbf{r}_x vector) in the presence of measurement error.

The *nugget* parameter can also be used to improve the stability of the kriging model. When superEGO is used for design optimization, points begin to cluster around the optimum (e.g., Figure 2(d)), making the \mathbf{R} matrix nearly singular and difficult to invert. In our implementation, a small nugget effect (e.g., 10^{-12}) is used to improve the conditioning without noticeably smoothing the data.

A simple one-dimensional example is shown to more easily visualize the smoothing effect. A uniformly distributed random number between $\pm \frac{1}{2}$ is added to the quadratic function $y = (x - 5)^2$, $x \in [0, 10]$. Nineteen sample points are taken: 11 equally spaced points and 8 additional points near the minimum. Using MLE, a kriging model is fit to $[\theta, p]$ for the interpolating and $[\theta, p, \text{nugget}]$ for the smoothing covariance models of Equations (3) and (10), respectively. Figure 3 shows the predicted value of the interpolating (solid line) and smoothed (dashed line) kriging models. In the area where the noise is prominent, the interpolating model oscillates in order to pass through each of the data samples, whereas the other model is much smoother in a least squares sense.

Figure 4 shows the kriging variance. For both the interpolating and smoothed models, the variance is lower in the middle because more data are available in that region. A consequence of the smoothing effect is that the variance model no longer returns to zero at the sample points. This is because the smoothing effectively increases the uncertainty in the model everywhere. In this example, there is little difference between the variance of the smoothed model at the sample points and the variance in locations far from the data. Because of this feature, one must be cautious when using Equation (7) as a measure of the uncertainty in smoothed kriging models. It is recommended that the interpolating covariance model of Equation (3) rather than Equation (10) be used in conjunction with Equation (7) for a more reliable estimate of the model uncertainty.

CASE STUDY

In this section the tools described above are used to create adaptive designs for an ergonomics experiment designed to explore the reach range of a seated test subject in a specific plane. A subjective measure of the *difficulty* of reaching a specific target is obtained. SuperEGO creates a model of the difficulty and adaptively controls the data to be gathered from the subject.

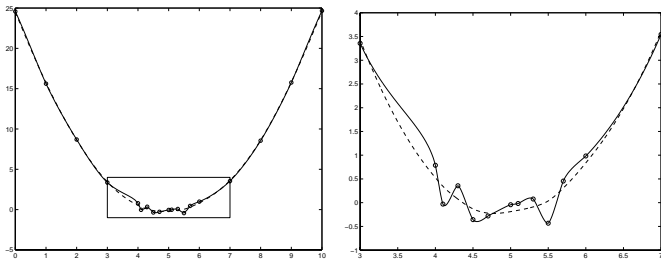


Figure 3. Kriging predictions for interpolating (solid) and smoothed (dashed) models (left). A close up of the boxed region is shown at right. Data points are shown as circles

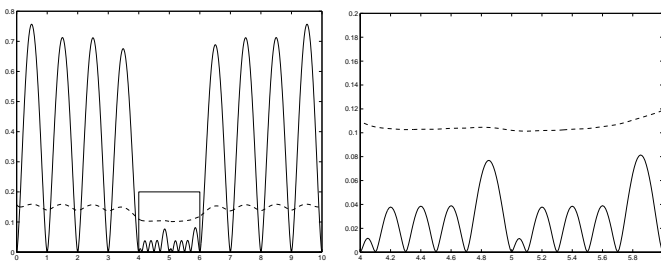


Figure 4. Kriging variance for interpolating (solid) and smoothed (dashed) models (left). A close up of the boxed region is shown at right.

Problem Description

Figure 5 shows the setup for the experiment. A subject is seated in a mock-up of an industrial or workplace environment, with the chair oriented so that the reach target is in the subject's lateral plane. A computer controlling the target can raise and lower it as well as move it nearer to or farther from the subject. In the testing procedure, the target is positioned and the subject is asked to reach to the target and depress the button for two seconds. The subject then rates the difficulty of the reach on a scale of 1 to 10, with 10 being the most difficult. Any target location that is unreachable is rated an 11. Maintenance of balance, the amount of exertion or degree of awkward posture required, and distance to the target all contribute to the difficulty of the reach.

The original testing procedure collects data along a finite number of rays. The length of the rays are calculated before the experiment by estimating the maximum reach length of the subject. The overall test procedure is done in multiple planes with multiple chairs and requires between 4 and 6 hours to complete. The goal of using adaptive sampling is to reduce the time required for subject testing by creating more efficient designs.

For simplicity, the pilot study shown here was restricted to two dimensions (i.e., a single plane) for the initial evaluation of the methodology. The 40 point sample for the ray-based approach is shown in Figure 6 for the 90° (lateral) plane. The plot is shown from a perspective behind a subject extending their right

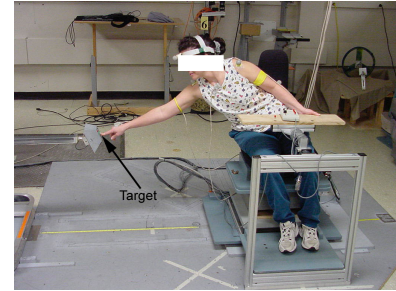


Figure 5. Example of a test subject reaching for the target

arm in a lateral motion. The $[0,0]$ reference is taken as the h-point, an ergonomic reference point at the mid-hip level along the body centerline.

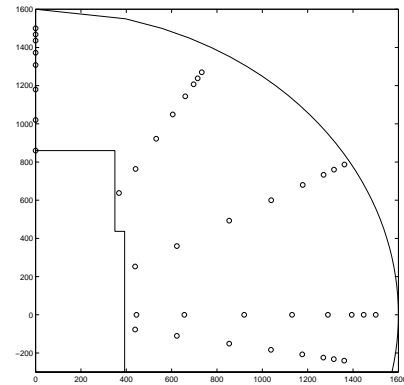


Figure 6. Example of ray-based experimental design

SuperEGO Implementation

Two test subjects were used for the experiment. Subject A was a 181 cm tall, 84 kg, 25 year-old male. Subject B was a 157 cm tall, 52 kg, 24 year-old female. Before any measurements were recorded, the subjects were each given about 10 reaches of various difficulty in order for them to begin building an internal system for assigning the reach effort value. Each subject was then given the same set of 11 initial sample point locations shown in Figure 7. The initial samples were selected to be somewhat space filling while including a number of points around the perimeter of the feasible space. It is a well known feature of kriging that the variance tends to be large around the outer edge of the design space which is less densely sampled. Populating points in this area at the onset aims to reduce the number of far away samples chosen after initialization.

The MLE fitting process of the kriging models is not very robust. Small changes in the data set can unpredictably lead to

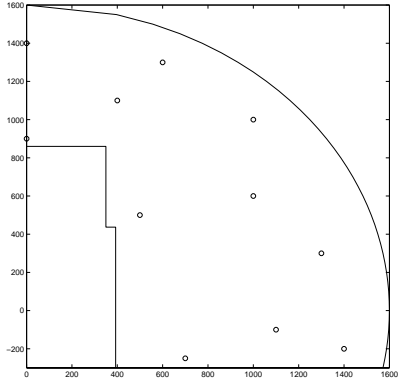


Figure 7. Initial set of 11 reaches

poor fits. For the case study, a kriging model of the subjects' perceived reach effort was successfully fit using the initial data set, then the model parameters $[\theta, p, nugget]$ were held fixed for the rest of the experiment. Doing so reduced the waiting time between reaches and yielded more reliable reach effort models. Fixing the covariance model parameters does not imply that the resulting kriging model is fixed. It will still change shape as data are added.

Three different sampling criteria were implemented in this study. The first attempted to create a space-filling design by selecting the location of maximum kriging variance, Equation (7), at each iteration. The other two criteria were used to increase the accuracy of the model where reach effort values were between 7 and 8, a region of interest to vehicle interior designers. This was accomplished by finding the maximum kriging variance for locations that had an estimated reach effort between 7 and 8. Points predicted to be outside the 7-8 zone were assigned an ISC value of zero. The difference between the last two criteria is that the first predicted the 7-8 zone using an interpolating kriging model, the latter a smoothing model. The ISC are summarized below.

$$ISC_1 = \hat{s}^2(\mathbf{x}) \quad (12)$$

$$ISC_2 = \hat{s}^2(\mathbf{x} | 7 \leq \hat{y}_{interpolating}(\mathbf{x}) \leq 8) \quad (13)$$

$$ISC_3 = \hat{s}^2(\mathbf{x} | 7 \leq \hat{y}_{smooth}(\mathbf{x}) \leq 8) \quad (14)$$

Three constraints were incorporated into the solution of the ISC problem at each iteration. They were the encroachment, out-of-reach, and predicted out-of-reach constraints. The first kept the target from getting too close to the subject and was represented by the rectangular region in the lower left corner of Figure 7. The out-of-reach constraints prevented placing the target in locations that were clearly out of reach of the subject, thus wasting time. The second constraint modeled the out-of-reach zone by a 1600 mm radius around the subject's h-point ($[0,0]$ on the

graph). The third constraint modeled the out-of-reach zone by a smoothed kriging model of the reach effort. Predicted reaches above 10 were considered infeasible. While g_3 is more adaptive to the subject, g_2 was kept as a redundancy in case the reach effort model were to behave erratically. The three constraints are summarized below.

$$g_1 : \mathbf{x} \notin \text{Encroachment zone} \quad (15)$$

$$g_2 : \|\mathbf{x}\| \leq 1600\text{mm} \quad (16)$$

$$g_3 : \hat{y}_{smooth} \leq 10 \quad (17)$$

During the experiments, the kriging variance of an *interpolating* model was used to quantify the uncertainty in reach effort model. While the smoothing approach exhibited a more well-behaved reach effort model, there were problems with the variance calculations as demonstrated in Figure 4. Because the sampling criteria used the kriging variance to create a space-filling design, it was critical that the variance tend toward zero at the sampled locations and increase monotonically as the distance from neighboring samples increased. Thus, the interpolating model was selected. However, we have taken advantage of the flexibility of superEGO to use smoothed kriging models as constraints while using the interpolating model to calculate variance estimates.

In summary, the following auxiliary optimization problem was solved for each iteration:

$$\max_{\mathbf{x}} ISC(\mathbf{x}) \quad (18)$$

subject to: $g_i(\mathbf{x})$ is feasible for all i

The solution to Equation (18) is the location to place the target next. The subject reached for the target and rated the effort. The \mathbf{R} matrix of the kriging model was then updated to incorporate the new data (without refitting the model parameters), and the process was repeated until a specified number of reaches were performed. For ISC_1 , a total of 30 points (including the initial 11) were sampled. Only 20 points were sampled for ISC_2 and ISC_3 .

Why Use Adaptive Sampling?

Before proceeding, it is first important to justify the need for adaptive sampling. To evaluate the efficacy of the adaptive sampling approach, an initial assessment was performed using analytical models to simulate the reach effort value a subject may assign for any given target location. Virtual subject A was a quadratic polynomial with a log term, virtual subject B a pure quadratic model. We compared the experimental design generated with superEGO against the static ray-based sample shown in Figure 6.

For each virtual subject, a kriging model was fit to a 40 point data sample collected at the locations specified by the ray-based approach shown in Figure 6. Another set of kriging models were fit to a smaller 30 point data sample collected using superEGO with both ISC_1 and ISC_2 , each initialized with 11 point sample of Figure 7. Because the virtual subjects were analytical functions, the RMS error from the predicted to the actual reach effort could be calculated for each kriging model.

Table 1 compares the model accuracy for the two subjects for the two sampling criteria. Test 1 computed the accuracy over the feasible space for the ray-based design and the adaptive design from ISC_1 . Test 2 computed the accuracy in only the 7-8 zone for the ray-based and adaptive design from ISC_2 . The adaptive sampling strategy provided superior global accuracy by using ISC_1 and provided more accurate results in the local zone of interest when ISC_2 was applied. In all cases, the model from a 30 point sample generated by superEGO was at least 3 times more accurate than the 40 point model generated by the ray-based approach. The advantages of adaptive sampling would likely be even more pronounced for a full three dimensional sampling.

Table 1. Comparison of RMS errors resulting from various sampling strategies. Measures of model accuracy are restricted to the feasible space for ISC_1 and to the 7-8 zone for ISC_2 .

	Virtual Subject A		Virtual Subject B	
	superEGO	ray-based	superEGO	ray-based
Test 1	1.31e-4	3.83e-4	2.07e-5	8.09e-4
Test 2	4.64e-5	2.73e-4	2.07e-5	1.08e-3

While these results do support the claim that adaptive sampling can lead to improved modeling accuracy, is the increased accuracy worth the complication? It would be much simpler to generate an efficient, space-filling design as a fixed DOE. Because the variation in the stature of test subject prohibits using a single DOE, one would have to scale the DOE for each subject. Doing so is not necessarily reliable because of the number of physical characteristics that determine reach range. Also, a subject may have physical limitations that prevent them from reaching a point that another person of the same size might easily reach. Thus, it is not feasible to create a scalable, static design that would fulfill the needs of this experiment. In addition, there may be an interest in subject-specific information to be accounted for in the sampling such as was done with ISC_2 . The adaptive sampling scheme is necessary in such cases. For these reasons, adaptive sampling has been selected as an appropriate tool for the test procedure.

Results

We begin by showing the resulting DOE's for each subject from ISC_1 (see Figure 8). The initial 11 points are shown as circles, with the remaining 19 infill points shown as x's. As expected, the two DOE's were quite different from each other. Theoretically, the kriging variance is homoscedastic, that is, it depends only on the location of the data, not the values thereof. So why then were the DOE's different? It is because the predicted out-of-reach constraint, g_3 , adapted to the user. As the kriging variance is high on the outer perimeter of the design space, where fewer data points are nearby, some infill points tended towards the edge of the feasible space. Because the predicted out-of-reach zone for Subject A was so large, g_3 was dominated by g_2 in the majority of the space, and points were placed along the edge of the 1600 mm radius. However, for Subject B, g_2 was dominated by g_3 and points were placed along the edge of her predicted out-of-reach zone, which was much smaller than the 1600 mm radius. Therefore, the infill locations for the two subjects quickly diverged. To compare the resulting reach effort models of the subjects after the 30 points, the interpolating and smoothed kriging models are shown in Figures 9 and 10, respectively.

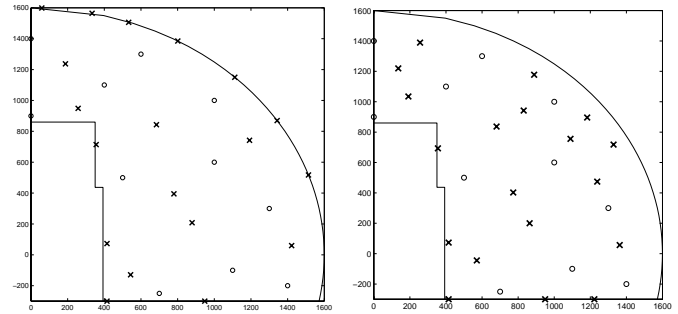


Figure 8. DOE for ISC_1 for Subjects A (left) and B (right). Circles and x's are initial and infill sample points, respectively.

The next two criteria were run for a total of 20 points each. Looking first at ISC_2 , Figure 11 shows the adaptive designs for the two subjects. For ISC_2 , the criterion estimates the 7-8 zone using the interpolating model. Figure 12 compares the predicted to the actual reach effort at each iteration. Similarly, Figures 13 and 14 show the adaptive designs and predicted vs. actual reach efforts for ISC_3 . For ISC_3 , the predicted 7-8 zone was estimated using the smoothing model. In both cases, the prediction accuracy was higher for Subject B than for Subject A. It is possible that the smaller feasible design space made predictions more reliable, but further work is being done to investigate this behavior.

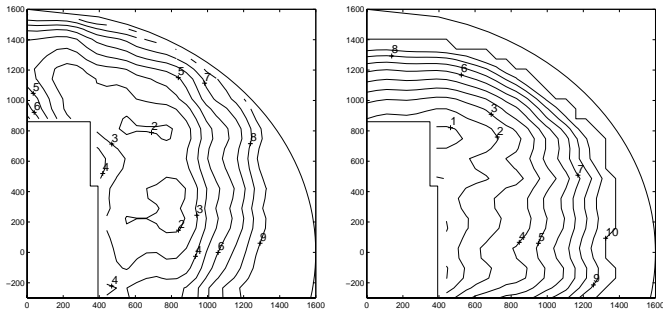


Figure 9. Reach Effort Interpolating Model for Subjects A (left) and B (right) based on DOE from ISC_1

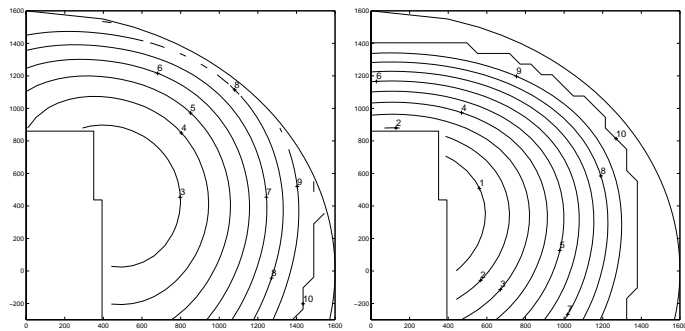


Figure 10. Reach Effort Smoothed Model for Subjects A (left) and B (right) based on DOE from ISC_1

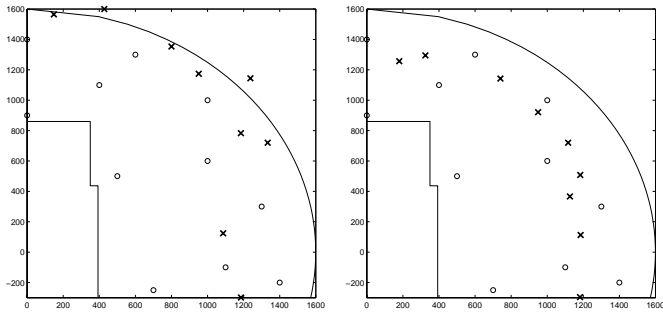


Figure 11. DOE from ISC_2 for Subjects A (left) and B (right). Circles and x's are initial and infill sample points, respectively.

CONCLUSIONS AND FUTURE WORK

A global constrained nonlinear optimization algorithm was used to create adaptive design of experiments. The generality and flexibility of the optimization algorithm lent itself well to exploring a variety of sampling criteria and constraint sets. It has been shown that the adaptive sampling successfully created experimental designs that adapted to the individual test subjects. For one subject, target locations were pushed further away be-

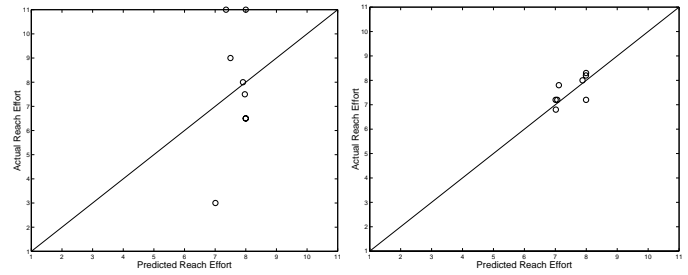


Figure 12. Comparison of predicted to actual reach effort using ISC_3 for subjects A (left) and B (right)

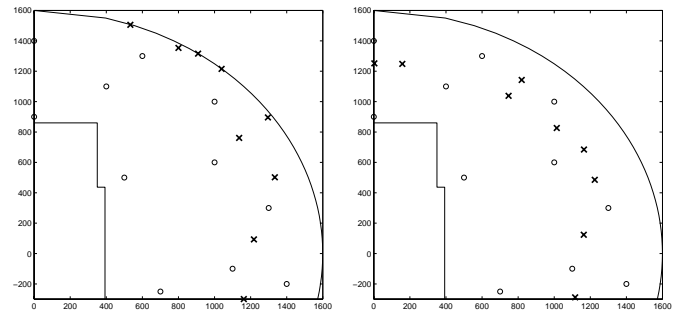


Figure 13. DOE from ISC_3 for Subjects A (left) and B (right). Circles and x's are initial and infill sample points, respectively.

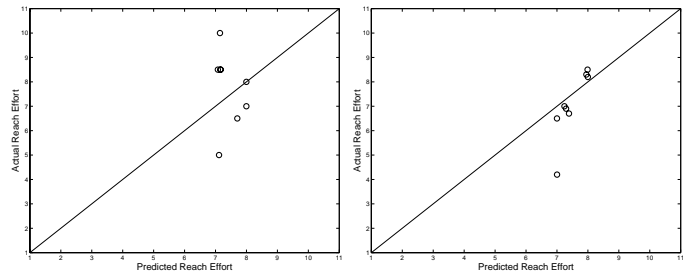


Figure 14. Comparison of predicted to actual reach effort using ISC_3 for subjects A (left) and B (right)

cause of his tall stature. For another, sample points were kept closer to the subject due to her shorter reach range. The integration of constraints into the solution of the ISC maximization problem allowed for irregularly shaped design spaces that took subject behavior into account. In addition, the ability to create smoothed kriging models was shown to be an important aid to the case study. The results of this pilot study have lead to some interesting possibilities.

Note from Figure 11 that two sample points for Subject A were taken outside the 1600 mm radius. For this particular experiment, g_2 was eliminated from the constraint set to explore

how well g_3 kept the samples within reach. The resulting DOE yielded 3 out-of-reach responses, compared to none for the ISC_3 experiment of Figure 13. While this does indicate that more targets were placed outside the subject's range, it did provide a reasonable constraint in that the subject was nearly capable of reaching the target. Eliminating g_2 may prove essential in some cases. For example, due to his height, Subject A was able to reach many of the targets placed along the 1600 mm radius. An experiment designed to search for an individual subject's maximum reach range would therefore be hindered by g_2 if the subject were tall enough. Attempting to scale the radius to the user may also prove ineffective because: A) it is difficult to accurately estimate someone's maximum reach a priori, and B) the maximum reach envelope is rarely a perfect circle. Adaptively setting the out-of-reach boundary via g_3 alone appears like a more appropriate method. A sampling criterion similar to those applied here could be used effectively with g_1 and g_3 to adaptively locate the maximum reach range.

Further work is currently underway to enhance the abilities of the smoothed kriging models. Rather than having a uniformly smoothed model, we have considered incorporating a measurement error that is a function either of the location in the design space or of the predicted value of the model. In this way, one could account for the fact that the subjects are more consistent when assigning very high or very low reach effort values than they are in assigning values in the medium range. The kriging model could potentially include more smoothing in the region of higher intrasubject variability and remain more true to the data at the extremes.

ACKNOWLEDGMENT

This research has been partially supported by the Automotive Research Center at the University of Michigan, a US Army Center of Excellence in Modeling and Simulation of Ground Vehicles and by the General Motors Collaborative Research Laboratory at the University of Michigan. This support is gratefully acknowledged. The authors would also like to thank the two test subjects for their patience and cooperation.

REFERENCES

- Atkinson, A., Hackl, P., and Müller, W., *Proceedings of MODA6: Model Oriented Data Analysis*, Physica Verlag, 2001.
- Atkinson, A., Pronzato, L. and Wynn, H.P. "MODA 5: Advances in model-oriented data analysis and experimental design: Proceedings of the 5th international workshop", 1998.
- Goovaerts, P., *Geostatistics for Natural Resources Evaluation*, Oxford University Press, New York, 1997.
- Hardwick, J.P. and Stout, Q.F., "Flexible Algorithms for Creating and Analyzing Adaptive Sampling Procedures", *New Developments and Applications in Experimental Design: Se-*

lected Proceedings of a 1997 Joint AMS-IMS-SIAM Summer Conference, (Eds. N. Flournoy, W.F. Rosenberger, and W.K. Wong), Institute of Mathematical Statistics, pp 91-105, 1998.

Flournoy, N., Rosenberger, W.F. and Wong, W.K., "New developments and applications in experimental design: Proceedings of the Joint AMS-IMS-SIAM Summer Research Conference", 1997.

Jones, D.R., Perttunen, C.D. and Stuckman, B.E., "Lipschitzian optimization without the lipschitz constant", *Journal of Optimization Theory and Application*, 79(1):157-181, 1993.

Jones, D.R., "The DIRECT Global Optimization Algorithm", *Encyclopedia of Optimization*, 1:431-440, 2001.

Montgomery, D.C., *Design and Analysis of Experiments, Fourth Edition*, J. Wiley & Sons, New York, 1997.

Sacks, J., Schiller, S.B., and Welch, W.J., "Design for Computer Experiments", *Technometrics*, 31:41-47, 1989.

Sacks, J., Welch, W.J., Mitchell, W.J., and Wynn, H.P., "Design and Analysis of Computer Experiments", *Statistical Science*, 4(4):409-435, 1989.

Sasena, M.J., *Flexibility and Efficiency Enhancements for Constrained Global Design Optimization with Kriging Approximations*, Ph.D. Thesis, University of Michigan, Dept. of Mech. Engr., 2002.

Sasena, M.J., Papalambros, P.Y. and Goovaerts, P., "Exploration of Metamodeling Sampling Criteria for Constrained Global Optimization", *Engineering Optimization*, to appear.

Sasena, M.J., Papalambros, P.Y. and Goovaerts, P., "The use of surrogate modeling algorithms to exploit disparities in function computation time within simulation-based optimization", *The Fourth World Congress of Structural and Multidisciplinary Optimization*, Dalian, China, 2001.

Schonlau, M., *Computer Experiments and Global Optimization*, Ph.D. Thesis, University of Waterloo, Waterloo, Canada, Dept. of Statistics, 1997.

Thompson, S.K. and Seber, G.A.F., *Adaptive sampling*, John Wiley & sons, 1996.

Zacks, S., "Adaptive Designs for Parametric Models", Eds. S. Ghosh and C.R. Rao, *Handbook of Statistics, Vol. 13*, Ch. 5, 1996.